



CHORUS

This is the accepted manuscript made available via CHORUS. The article has been published as:

Spatial Interactions and Oscillatory Tragedies of the Commons

Yu-Hui Lin and Joshua S. Weitz

Phys. Rev. Lett. **122**, 148102 — Published 12 April 2019

DOI: [10.1103/PhysRevLett.122.148102](https://doi.org/10.1103/PhysRevLett.122.148102)

Spatial interactions and oscillatory tragedies of the commons

Yu-Hui Lin¹ and Joshua S. Weitz^{2,1}

¹*School of Physics, Georgia Institute of Technology, Atlanta, GA, USA*

²*School of Biological Sciences, Georgia Institute of Technology, Atlanta, GA, USA*

(Dated: March 20, 2019)

A tragedy of the commons (TOC) occurs when individuals acting in their own self-interest deplete commonly-held resources, leading to a worse outcome than had they cooperated. Over time, the depletion of resources can change incentives for subsequent actions. Here, we investigate long-term feedback between game and environment across a continuum of incentives in an individual-based framework. We identify payoff-dependent transition rules that lead to oscillatory TOC-s in stochastic simulations and the mean field limit. Further extending the stochastic model, we find that spatially explicit interactions can lead to emergent, localized dynamics, including the propagation of cooperative wave fronts and cluster formation of both social context and resources. These dynamics suggest new mechanisms underlying how TOCs arise and how they might be averted.

Introduction—In 1968, Garrett Hardin explored a social dilemma, which he termed the ‘Tragedy of the Commons’ (TOC) [1]. The social dilemma arises when two individuals choose amongst distinct strategies to utilize a limited public good. Both individuals receive the maximal combined benefit if they utilize the public good with restraint, *i.e.*, if they ‘cooperate’. However, each individual receives the maximal personal benefit if they utilize the public good without restraint, *i.e.*, if they ‘defect’, while their opponent cooperates. As a consequence, individuals acting rationally will cheat leaving all worse off. Hardin argued that such a TOC is inevitable [1].

Evolutionary dynamics arising from a TOC dilemma can be modeled in terms of changes in the frequencies of individuals from two populations. Individuals interact and receive payoffs that depend on their strategy and the strategy of their opponent [2]. In replicator dynamics [3], the payoff represents a relative fitness which determines the growth of cooperators, with frequency x , and of defectors, with frequency $1 - x$, *i.e.*,

$$\dot{x} = x(1 - x)(r_C(x, A) - r_D(x, A)). \quad (1)$$

The values r_C and r_D denote the context-dependent fitness payoff to cooperators and defectors respectively, given the payoff matrix $A = \begin{bmatrix} R & S \\ T & P \end{bmatrix}$, where $r_C = Rx + S(1 - x)$, $r_D = Tx + P(1 - x)$, such that R denotes the reward to cooperation, T denotes the temptation to cheat, S denotes the sucker’s payoff, and P denotes the punishment given mutual defection. A TOC occurs when $T > R$, $P > S$, and $P < R$. However, in contrast to standard game theory assumptions, payoffs are unlikely to remain fixed after repeated decisions that degraded commonly-held resources.

To address this issue, a recent model [4] considered dynamics arising given resource-dependent payoff matrices $A(n) = A_0(1 - n) + A_1(n)$, which interpolate between A_0 and A_1 , the payoff matrices given deplete and replete resource states, respectively, *i.e.*, $A(n) = \begin{bmatrix} R_0 & S_0 \\ T_0 & P_0 \end{bmatrix}(1 - n) + \begin{bmatrix} R_1 & S_1 \\ T_1 & P_1 \end{bmatrix}n$. This model of coevolutionary game dynamics included feedback with the environmen-

tal state denoted by $0 \leq n \leq 1$, such that

$$\epsilon \dot{x} = x(1 - x)[r_C(x, A(n)) - r_D(x, A(n))], \quad (2)$$

$$\dot{n} = n(1 - n)(\theta x - (1 - x)). \quad (3)$$

where ϵ is a speed parameter and θ denotes the strength of cooperators in restoring the environment. In this coevolutionary model, the payoff matrices A_0 and A_1 can have markedly different Nash equilibria [5]. For example, when defection is uniformly favored when $n = 1$ and cooperation is favored when $n = 0$, then the the system can exhibit a novel phenomenon termed an ‘oscillatory tragedy of the commons’ (o-TOC). An o-TOC denotes a trajectory in the phase plan that approaches a heteroclinic cycle. Given a replete environment, the population rapidly switches from cooperation to defection, which then degrades the environment. In the depleted environment, cooperators re-establish, improving the environment, then defectors invade and the cycle repeats. Other outcomes, including a TOC and the aversion of a TOC can emerge given other payoff matrices [4].

Individual-based coevolutionary game—This coevolutionary game model is the basis for our development and analysis of an individual-based framework to assess the influence of noise (first) and spatially explicit interactions (second) on the emergent dynamics of social context and resources. To begin, consider a system comprised of n_C cooperators and n_D defectors, such that $N = n_C + n_D$. A single time step consists of N events. In each event, a randomly chosen individual (the focal player) interacts with another individual (the opponent) chosen at random. The payoff to the focal player influences its probability to reproduce. Critically in our proposed framework, successful reproduction by the focal player replaces a randomly chosen *third* individual (see [6] for a related public goods model that decouples interaction and reproduction). The following reactions denote those transitions that lead to a change in the number of cooperators

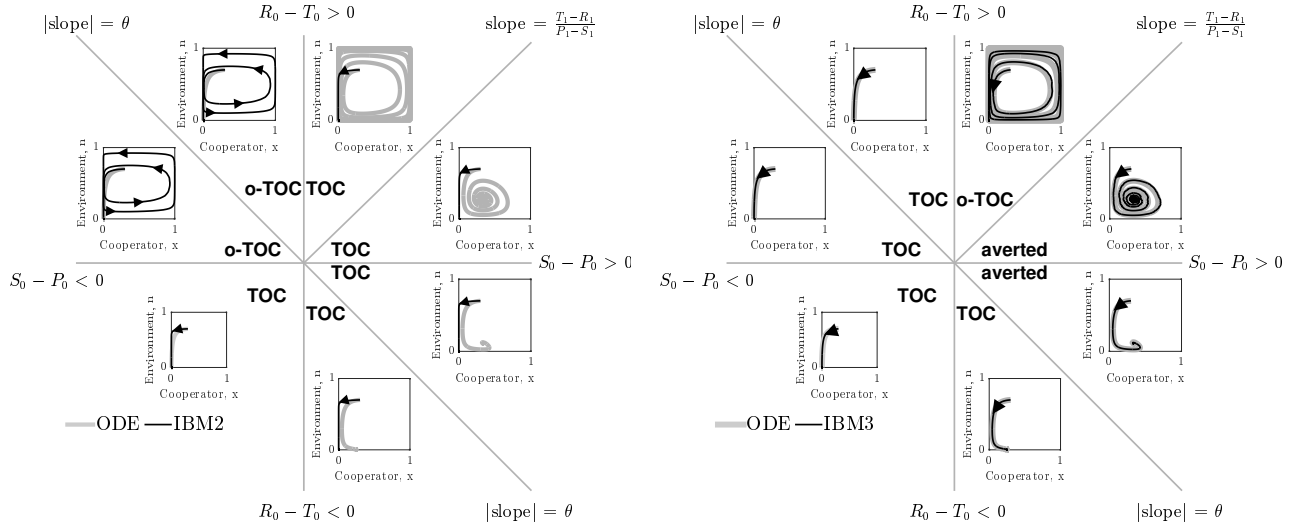
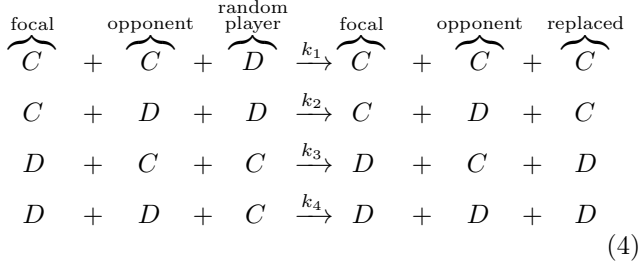


FIG. 1. Coevolutionary dynamics of strategies and resources in replicator and IBM dynamics. (left) The dynamics with ‘IBM2’, in which offspring of the focal player replace the opponent. (right) The dynamics with ‘IBM3’, in which offspring of the focal player replaces a random individual. In both panels, parameter space is divided according to the sign of $R_0 - T_0$, $S_0 - P_0$. In each section in the parameter space, a phase diagram with different A_0 in is shown, where the x-axis represents x and the y-axis denotes n . Light gray trajectories are mean field solutions and black trajectories denote IBM dynamics where arrows denote the flow of time. Visualized IBM trajectories are the average of 100 replicates with the same parameter set, except for oscillatory dynamics, given phase differences that can arise due to demographic noise. Common parameters for all replicates: $\theta = 2$, $\epsilon = 0.5$, $\Delta x = 1$, and $\Delta t = 0.05$, $A_1 = [3, 0; 5, 1]$; A_0 varies by region. Full parameter list for A_0 in Fig. S1.

or defectors:



where k_i denote reproduction rates.

In the three-individual framework, the master equation for the dynamics of cooperators is:

$$\begin{aligned}
 \mathbb{P}(n_C, \tau + \Delta\tau) &= \mathbb{P}(n_C, \tau) + \mathbb{T}(n_C | n_C - 1) \mathbb{P}(n_C - 1, \tau) \Delta\tau \\
 &+ \mathbb{T}(n_C | n_C + 1) \mathbb{P}(n_C + 1, \tau) \Delta\tau \\
 &- \mathbb{T}(n_C + 1 | n_C) \mathbb{P}(n_C, \tau) \Delta\tau \\
 &- \mathbb{T}(n_C - 1 | n_C) \mathbb{P}(n_C, \tau) \Delta\tau + \mathcal{O}(\Delta\tau^2),
 \end{aligned} \quad (5)$$

where the transition rates are:

$$\begin{aligned}
 \mathbb{T}(n_C + 1 | n_C) &= k_1 n_C \frac{n_C - 1}{N - 1} \frac{n_D}{N - 1} + k_2 n_C \frac{n_D}{N - 1} \frac{n_D}{N - 1} \\
 \mathbb{T}(n_C - 1 | n_C) &= k_3 n_D \frac{n_C}{N - 1} \frac{n_C}{N - 1} + k_4 n_D \frac{n_D - 1}{N - 1} \frac{n_C}{N - 1}.
 \end{aligned} \quad (6)$$

In the SI, we derive the expected mean field dynamics for the frequency of cooperators $x \equiv \lim_{N, n_c \rightarrow \infty} \left(\frac{n_C}{N} \right)$ from the master equation:

$$\dot{x} = x(1-x) [(k_1 - k_3)x + (k_2 - k_4)(1-x)]. \quad (7)$$

We recover the replicator dynamics of the coevolutionary model when $k_1 = R(n)$, $k_2 = S(n)$, $k_3 = T(n)$, and $k_4 = P(n)$. Hence, transition rates are a function of resource- and social-context dependent payoffs. In contrast, mean field dynamics derived via a two-player individual based model formulation (IBM2) result in a logistic dependency on x distinct from the cubic nonlinearity in Eq. 7 (see SI for derivation and details).

Effect of demographic noise— In order to further evaluate stochastic dynamics of the IBM formulation, we simulated the joint dynamics of resources n and social context x using $N = 10^4$ individuals. A single time step over an interval Δt includes N game steps followed by changes in resource levels, $n(t)$ according to Eq. 3 (see Supplementary Information (SI) for details). Hence, in this formulation stochasticity is introduced only at the level of the individuals. Given the master equation analysis, we define reproduction rates k_i based on the current environmental state $n(t)$. Consistent with our finding from the master equation, the simulation results of the individual-based model involving three players (IBM3) recapitulate predictions of the mean-field replicator dynamics model (see FIG. 1-right). Specifically, we identify seven distinct phases corresponding to the relative magnitude of payoffs given the resource deplete state. The phases and their asymptotic behavior agree qualitatively with mean-field predictions. In contrast, if the focal player reproduces and replaces the opponent (which we term IBM2, as is often assumed in two-player variants of spatial games), then the individual-based simulations diverge from predictions (see FIG. 1-left) as anticipated from expected mean field dynamics (see SI).

There are two notable quantitative differences in the IBM3 simulations with respect to predictions from replicator dynamics. First, whereas mean-field dynamics predict convergence to a heteroclinic cycle (see ‘o-TOC’ region in FIG. 1-right), the IBM simulations stochastically reach an absorbing state on the boundary. Such a result is anticipated in any finite size simulation, given that heteroclinic cycles asymptotically approach the boundary. Second, the mean field model predicts closed periodic orbits given certain symmetric properties of A_0 and A_1 (corresponding to the line with slope $(T_1 - R_1)/(P_1 - S_1)$ in FIG. 1-right.) In contrast, the IBM simulations have demographic noise, which can lead to repeated oscillations and convergence to a boundary (see FIG. S3).

Demographic noise and spatial structure—To study the combined effects of spatial structure and demographic noise (see [7]) we extended the IBM3 framework to a 2-dimensional fully occupied lattice with L sites per dimension given periodic boundary conditions, where the $N = L^2$ individuals are either cooperators or defectors. The focal player is selected at random and the opponent is chosen randomly from the von Neumann neighborhood of the focal player. We denote the position of the focal player (opponent) as \vec{r}_F (\vec{r}_O). The focal player reproduces with probability rate $k_m(s_F, s_O, \bar{n})$ given the strategy set of focal player and opponent, s_F and s_O , and the average local environment, $\bar{n} = (n(\vec{r}_F) + n(\vec{r}_O))/2$. Environmental state dynamics $n(\vec{r}, t)$ are augmented by diffusion, i.e.,:

$$\frac{\partial n}{\partial t} = n(1 - n)(\theta x - (1 - x)) + D_n \nabla^2 n. \quad (8)$$

The diffusivity D_n controls the redistribution of resources relative to population dynamics. In the case of finite diffusion, the corresponding partial differential equation is replaced by its spatially discretized version (see SI).

Simulations of coevolutionary game-environmental dynamics reveal dramatic changes in outcomes given spatially explicit interactions. FIG. 2 compares dynamics of non-spatial and spatial IBM models with three different diffusivities, $D_n = 0, 1, \infty$, classifying outcomes based on whether there is a TOC or not (the latter we term averted, see SI for criteria). The heat maps show the proportion of averted cases among all replicates. Spatial interactions enable TOC aversion when cooperation is favored given a coordination game context ($R_0 > T_0$ and $S_0 < P_0$, see upper left). However, spatial interactions also restrict the parameter regimes where a TOC can be averted given an anti-coordination game context ($R_0 < T_0$ and $S_0 > P_0$, see bottom right). For long-term dynamics, we find that oscillating dynamics are typical in $D_n = \infty$ cases (see examples in the SI). Such oscillatory dynamics can spiral inwards when TOC-s are averted or outwards to the boundary. Of note, amongst IBM models we only observe a persistent o-TOC when $D_n = \infty$; indicating the role of strong spatial coupling to induce oscillations.

Spatiotemporal dynamics with environmental

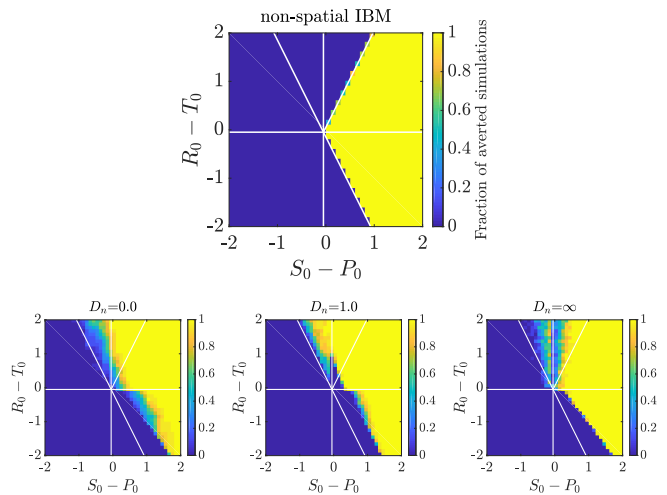


FIG. 2. Strategy-resource dynamics given spatial interactions. Colors in each heat-map denote the fraction of averted dynamics out of 20 replicates with different A_0 's. The horizontal axis of the heat maps are $S_0 - P_0$ and the vertical ones are $R_0 - T_0$. Each grid on the heat maps has increment 0.1. The diffusivity D_n is shown in the title of each panel. Other parameters for all replicates are $L = 100$, $\theta = 2$, $\epsilon = 0.5$, $\Delta x = 1$, and $\Delta t = 0.05$, $A_1 = [3, 0; 5, 1]$. The white lines mark out the boundary of different dynamics predicted by the mean field model. Full parameter list for A_0 in Fig. S2.

diffusion—We further investigated spatiotemporal dynamics focusing on variation in D_n given parameter regimes with both averted and TOC dynamics. These regimes correspond to the case where $S_0 < P_0$, $R_0 > T_0$ and where $R_0 > -\theta(S_0 - P_0) + T_0$ (see bottom panels of FIG. 2). The results of spatially explicit IBM3 model simulations are shown in FIG. 3 for $D_n = 0, 1$ and ∞ . Notably, all cases appear to exhibit clustering amongst cooperators and the cases with heterogeneous environmental dynamics ($D_n = 0$ and $D_n = 1$) also appear to exhibit clustering between cooperators and environmental resource state. However, there are markedly different types of emergent spatial patterns give variation in the diffusivity of environmental resource state. In order to assess clustering quantitatively, we analyzed the joint structure of social context and resource levels by measuring the spatial cross-correlation function:

$$g_{CN}(r, t) = \frac{L^2}{\mathcal{A}(r)} \frac{\sum_{i,j} (\sum_{i',j'} x_{i,j}(t) \cdot n_{i',j'}(t))}{\sum_{i,j} x_{i,j}(t) \sum_{i,j} n_{i,j}(t)}, \quad (9)$$

and the spatial autocorrelation function of cooperator clustering:

$$g_{CC}(r, t) = \frac{L^2}{\mathcal{A}(r)} \frac{\sum_{i,j} (\sum_{i',j'} x_{i,j}(t) \cdot x_{i',j'}(t))}{(\sum_{i,j} x_{i,j}(t))^2}, \quad (10)$$

where $r < \sqrt{(i - i')^2 + (j - j')^2} \leq r + 1$, and $\mathcal{A}(r)$ denotes the number of lattice sites within this range in both cases. We then fit the short-range components of the observed correlation at a fixed time point to a decaying exponential, i.e., $g(r, t) \sim 1 + \alpha(t)e^{-r/\xi(t)}$ given pre-factor α and correlation length ξ .

The spatial autocorrelation analysis confirms the emergence of clustering amongst cooperators when the TOC is averted, i.e., $g_{CC}(r) > 1$ for $r \rightarrow 1$ (see black lines in the sub-panels of FIG. 3). Yet there are marked differences in the dynamics of the cross-correlation between cooperators and the environmental state.

For $D_n = 0$, the environment and cooperative population propagate outward as a wave. The cooperative population spreads leaving patches of resource replete environments. The $g_{CN}(r)$ plots shows that x and n can be positively correlated as a wave initiates but negatively correlated once defectors invade and replace resource replete environments, leading to (often disjoint) patchy distributions of both resources and cooperators. In contrast, for $D_n = 1$, small clusters of cooperators and localized resources form after initial transient dynamics. This feature is captured by the $g_{CN}(r)$ analysis, revealing strongly elevated cross-correlation (see the middle row of FIG. 3) as well as similar pattern in the dynamics of $g_{CC}(r)$ and $g_{CN}(r)$. We note that these ‘gangs’ of cooperators and their environmental ‘tail’ are chased by a dominant group of defectors (see [8] for related findings in evolutionary PD models without environmental feedback). Finally, given $D_n = \infty$, the resources are uniform across space. Cooperative clusters grow towards system sizes due to the strong spatial coupling mediated via fast resource diffusivity. The single large cooperator cluster expands and shrinks over time with increasing amplitude, as evidenced by the elevated autocorrelation of $g_{CC}(r)$ in the bottom row of FIG. 3, with rapid switches in resource state, leading to an eventual collapse of the cooperator population. We do not report $g_{CN}(r)$ given the uniform distribution of resources given $D_n = \infty$.

Discussion—In summary, we have developed an individual-based framework to incorporate the effects of demographic noise and spatial interactions [7] in coevolutionary game dynamics that couple individual strategies and the environment. The IBM involving three players in a game recapitulates and generalizes earlier findings from a coevolutionary game model, including the emergence of an oscillatory tragedy of the commons [4]. Spatial interactions can shift the domains in which a tragedy of the commons may arise when compared to non-spatial models [9]. Spatially explicit dynamics also lead to novel, coherent spatiotemporal patterns [10–14], including diffusive clusters, flickering, and wave-like patterns. These joint dynamics of resources and social strategies suggest multiple avenues for future study, including formally deriving effective PDEs to characterize whether the system permits propagating waves in the large system limit. It will also be critical to evaluate the extent to which spatial interactions modify strategy-environment feedback in proposed generalizations [15] of the replicator framework underlying the present work [4] and in stochastic games with feedback between behavior and public good states [16]. Finally, the spatial framework developed here may also aid efforts to understand how microorganisms produce and utilize public goods, *e.g.*, siderophores – ex-

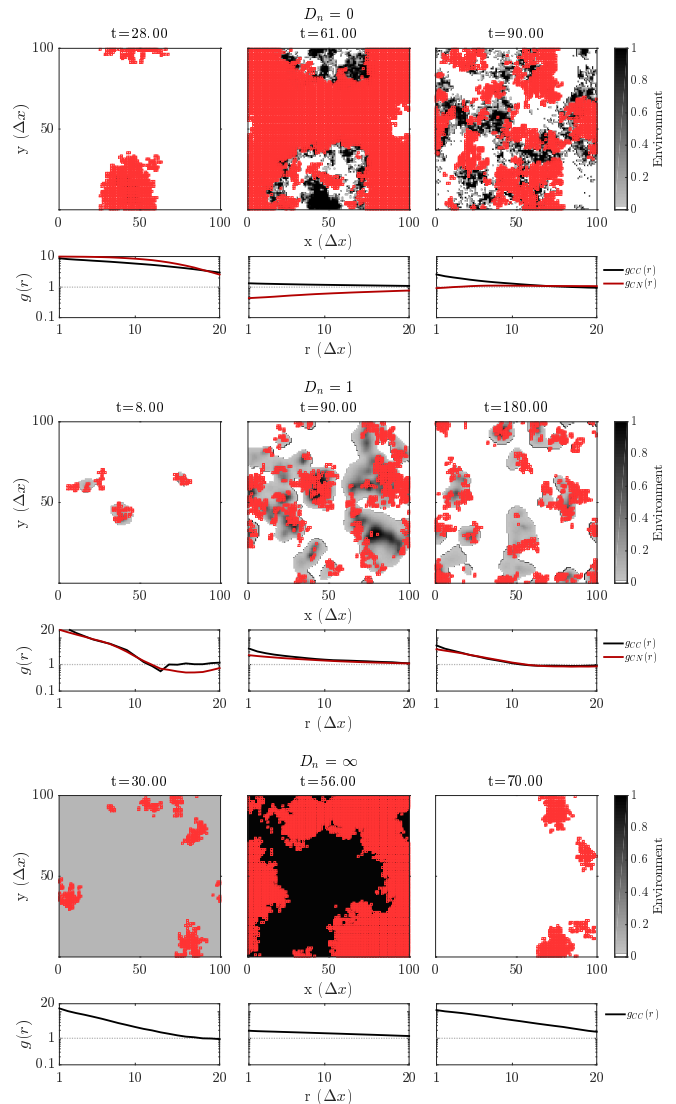


FIG. 3. Spatiotemporal dynamics of resources and cooperation. The background color represents the environment, while a red square means a cooperator occupies the lattice site. The empty sites are occupied by defectors. (Top row) $D_n = 0$, a circular wave of cooperative population propagates outward. (Middle row) $D_n = 1$, a few small patches of cooperators move around and divide. (Bottom row) $D_n = \infty$, a large cooperator cluster expands and shrinks over time with increasing amplitude until extinction.

tracellular iron harvesting enzymes, as but one example of many [6, 17–23]. Given increasing pressures on limited resources, we intend to leverage prior work on controlling mean-field strategy-environment dynamics [24] to identify ways in which local manipulation of resources, strategies, and/or perceptions can help stabilize and conserve the commons.

ACKNOWLEDGEMENTS

We thank Erol Akçay, Marianne Bauer, Ceyhun Eksin, Guanlin Li, Keith Paarporn, William Ratcliff, and Peter Yunker for feedback and Stephen Beckett for reviewing code. This work was supported by the Simons Foundation (SCOPE award ID 329108, J.S.W.) and by Army Research Office grant W911NF-14-1-0402.

-
- [1] G. Hardin, *Science* **162**, 1243 (1968).
- [2] J. M. Smith and G. R. Price, *Nature* **246**, 15 (1973).
- [3] M. A. Nowak, *Evolutionary Dynamics* (Harvard University Press, 2006).
- [4] J. S. Weitz, C. Eksin, K. Paarporn, S. P. Brown, and W. C. Ratcliff, *Proceedings of the National Academy of Sciences* **113**, E7518 (2016).
- [5] J. F. Nash Jr, *Econometrica: Journal of the Econometric Society*, 155 (1950).
- [6] M. Bauer and E. Frey, *Physical Review E* **97**, 042307 (2018).
- [7] R. Durrett and S. Levin, *Theoretical Population Biology* **46**, 363 (1994).
- [8] G. Szabó and C. Tóke, *Physical Review E* **58**, 69 (1998).
- [9] J. Halatek and E. Frey, *Nature Physics* **14**, 507 (2018).
- [10] M. A. Nowak and R. M. May, *Nature* **359**, 826 (1992).
- [11] T. Butler and N. Goldenfeld, *Physical Review E* **80**, 030902(R) (2009).
- [12] T. Butler and N. Goldenfeld, *Physical Review E* **84**, 011112 (2011).
- [13] M. A. Nowak and R. M. May, *International Journal of Bifurcation and Chaos* **3**, 35 (1993).
- [14] M. Nanda and R. Durrett, *Proceedings of the National Academy of Sciences* **114**, 6046 (2017).
- [15] A. R. Tilman, E. Akçay, and J. Plotkin, *bioRxiv* (2018), 10.1101/493023.
- [16] C. Hilbe, Š. Šimsa, K. Chatterjee, and M. A. Nowak, *Nature* **559**, 246 (2018).
- [17] O. X. Cordero, L.-A. Ventouras, E. F. DeLong, and M. F. Polz, *Proceedings of the National Academy of Sciences* **109**, 20059 (2012).
- [18] R. Niehus, A. Picot, N. M. Oliveira, S. Mitri, and K. R. Foster, *Evolution* **71**, 1443 (2017).
- [19] R. Menon and K. S. Korolev, *Physical Review Letters* **114**, 168102 (2015).
- [20] O. Lewin-Epstein, R. Aharonov, and L. Hadany, *Nature Communications* **8**, 14040 (2017).
- [21] W. Lee, M. van Baalen, and V. A. Jansen, *Journal of Theoretical Biology* **388**, 61 (2016).
- [22] S. A. West and A. Buckling, *Proceedings of the Royal Society of London. Series B: Biological Sciences* **270**, 37 (2003).
- [23] S. A. West, S. P. Diggle, A. Buckling, A. Gardner, and A. S. Griffin, *Annual Review of Ecology, Evolution, and Systematics* **38**, 53 (2007).
- [24] K. Paarporn, C. Eksin, J. S. Weitz, and Y. Wardi, *IEEE Conference on Decision and Control (CDC) 2018* (2018), 10.1109/CDC.2018.8619604.